



Investigation of sound and vibration behavior of cylindrical gears

A. Beinstingel^{1,2} · F. Haringer² · W. Sigmund² · M. Heider² · B. Pinnekamp² · S. Marburg¹

Received: 27 March 2023 / Accepted: 13 July 2023 / Published online: 31 July 2023
© The Author(s) 2023

Abstract

As technology progresses, the demands placed on drive trains are continuously increasing. This also includes the vibration behavior and the acoustic performance of gearboxes. Especially when electric motors are used for propulsion and thus masking by an internal combustion engine or a similar driving machine vanishes, the optimization of the noise characteristics contribute as an important aspect to a successful gear design. Since the main noise originates from the characteristic power transmission process of the mating gear teeth, the transfer path of the structure-borne sound is a complex composition of gear mesh, shafts, bearings and housing. As a result, the acoustic performance depends on various influencing factors and hence a deep understanding of the dynamic interactions in a gearbox is required for optimization purposes. A suitable calculation strategy highly supports production development by identifying key influencing factors. In this context, the investigation of the dynamic behavior of a gearbox concept with respect to its acoustic performance is presented in this article.

Untersuchung des Geräusch- und Schwingungsverhaltens von Stirnrädern

Zusammenfassung

Im Zuge des technischen Fortschritts steigen die Anforderungen an den Antriebsstrang kontinuierlich an. Dazu gehört auch das Schwingungsverhalten und die akustische Qualität von Getrieben. Insbesondere wenn Elektromotoren zum Antrieb eingesetzt werden und damit die Maskierung durch einen Verbrennungsmotor oder eine ähnliche Antriebsmaschine entfällt, trägt die Optimierung des Geräuschverhaltens als wichtiger Aspekt zu einer erfolgreichen Getriebeauslegung bei. Da das Hauptgeräusch durch den charakteristischen Kraftübertragungsvorgang der Verzahnung entsteht, ist der Übertragungsweg des Körperschalls eine komplexe Zusammensetzung aus Zahneingriff, Wellen, Lagern und Gehäuse. Dies hat zur Folge, dass das akustische Verhalten von verschiedenen Einflussfaktoren abhängt und somit ein tiefes Verständnis der dynamischen Wechselwirkungen in einem Getriebe zu Optimierungszwecken erforderlich ist. Eine geeignete Berechnungsstrategie unterstützt die Produktentwicklung in hohem Maße. In diesem Zusammenhang wird in diesem Artikel die Untersuchung des dynamischen Verhaltens eines Getriebekonzepts in Bezug auf die akustische Perfomanz vorgestellt.

1 Introduction

In modern power transmission systems, noise contributes as a quality feature to the success of a gearbox design. It is known that the power transmission process leads to an

internal vibration excitation due to the continuously changing contact conditions of the mating gear teeth. This periodic characteristic creates oscillating torque and forces on the shafts and thus also on the bearings [1]. A subsequent transmission to the housing produces two decisive vibration outputs: the radiation of air-borne noise at the housing surfaces and a transportation of the structure-borne sound to the adjacent components. An improved gear tooth design is the primary measure to achieve quiet operation. However, as technology progresses, the acoustic demands on gearboxes are continuously increasing and hence secondary measures are becoming necessary to ensure optimal acoustic performance. In this context, a deep understanding of the arising

✉ A. Beinstingel
andreas.beinstingel@tum.de

¹ Chair of Vibroacoustics of Vehicles and Machines, Technical University of Munich, 85748 Garching n. Munich, Germany

² RENK GmbH, Goegginger Str. 73, 86159 Augsburg, Germany

dynamics is required to control the mechanical properties in a positive way.

Especially when the production and optimization of a prototype is not a feasible option, an appropriate simulation strategy is of major importance. Accordingly, the investigation of gear dynamics has been a great research topic for decades [2–5] and is still ongoing [6–8]. Nevertheless, the literature is quite sparse with respect to acoustic efforts in order to consider the complete transfer path that occurs in a gear system regarding the expected noise emission level. An initial example with this acoustic motivation is available in [9] and a similar simulation strategy is applied in [10]. Both works focus on a total system analysis to determine the resulting noise radiation of a single-stage gearbox in three-dimensional space. The computational approach is split in each case into two simulation steps. First, the dynamics of the addressed gearboxes are investigated in the time domain to account for nonlinear interactions. To speed up computation time, the housing is considered initially in a reduced form by a compliance matrix approach. Then, in a subsequent step, the derived dynamic bearing forces (i.e., the result of the previous simulation step) serve as the basis for a linear computation of the full housing structure in the frequency domain by considering them as external excitation loads at the corresponding bearing stations. Finally, the distribution of the sound pressure level (SPL) in the surrounding fluid domain is determined to complete the investigation of the vibro-acoustic propagation in a gear-bearing-housing-system [10]. A numerically efficient alternative for the first solution step, based on the harmonic balance method (HBM) [11], is presented more recently in [12] and in [13]. Additionally, the housing structure is taken into account by a component mode synthesis (CMS) in the sense of [14]. As a result, all dynamic cross-influences are considered nonlinear in the form of a coupled gear-shaft-bearing-housing-system in three-dimensional space. The selected modeling approach in [13] seems to be appropriate as the simulation is validated by a measurement of the housing accelerations of a two-stage double-helical gearbox with large component dimensions. Therefore, a quantitative prediction of the equivalent radiated power (ERP) [15, 16], as a part of this first solution phase, is reasonable. Thus, the presented strategy in [13] is applied in this paper to investigate the sound and vibration behavior of a single-stage gearbox for a certain purpose in a marine application. On top, the actual sound power as well as the radiated SPL of one gearbox concept is investigated by means of the boundary element method (BEM) [17] in order to get an impression of the informative power of the ERP statement.

This article is structured as follows: At first, the basic modeling approach of [13] is briefly reviewed and minor adjustments are introduced regarding the CMS of the hous-

ing structure. Additionally, the fundamentals of the implemented simulation approach regarding the BEM for the acoustic post-processing are specified. Then, an application example in terms of a single-stage gearbox concept is presented for a ship propulsion system. In total, four alternative gearbox designs for a certain purpose are focused and the corresponding simulation results are discussed in a subsequent section. Here, the ERP is first compared to the BEM solution and then serves as the evaluation parameter for the case study. Finally, conclusions and findings are summarized in the closing section.

2 Computational modeling technique

The underlying computational model for the upcoming investigation within the corresponding simulations is explained in detail in [13]. Here, the shafts are described by linear rotating beam elements [18, 19]. The shear coefficient with respect to Timoshenko's theory is derived appropriately in accordance to [20] for each shaft section. The support of these rotating beam elements against the housing structure and vice versa is considered nonlinear in form of a fluid-structure-interaction (FSI) as slide bearings are used in this application. Here, the dynamic behavior of the corresponding oil pressure in each bearing is described in terms of lubrication theory [21]. The numerical solution of the associated Reynold's equation is carried out with the finite element method (FEM) as described in [22]. This computation is performed in each iteration at isothermal temperature conditions. For efficiency reasons, cavitation is considered as suggested by Gumbel [23]. The gear mesh algorithm is established as a nonlinear hybrid analytical-numerical contact formulation, which is described in detail in [24, 25]. Here, the iterative procedure makes use of a compliance matrix approach to speed up computation time. This procedure is similar to common approaches [26–30], excluding the initial derivation step of the underlying tooth compliances. This specific determination strategy is based on the elastic deformation behavior of a three-dimensional continuum of a single pair of teeth. The numerical representation is based on the Isogeometric Analysis (IGA) [31] and hence allows to account for the exact tooth geometry. As a result, the elastic deformation properties of the gear teeth are considered with high precision. An up-to-date summary of different modeling techniques with respect to the determination of the gear mesh stiffness is available in [32]. However, the applied approach accounts also for the Hertzian contact deformation in accordance to [33]. In addition to the iterative response to the dynamic deflections of the surrounding components, possible mesh interference [34, 35] (e.g., a premature mesh engagement), manufacturing deviations (e.g., shaft misalignment) as well as profile

modifications may influence the power transmission process during simulation. Here, the nonlinear update strategy of the gear engagement scenario covers highly detailed the current contact conditions along the complete face width for each specific rolling position. A constant damping is defined for the gear meshing process with respect to [36]. In contrast, the damping effect of the slide bearings is covered automatically by the FSI. The material damping of the rotating beam elements as well as the housing structure is achieved in form of a Rayleigh damping [37].

As the geometry of a housing structure is usually quite complex, the FEM is applied to describe this dynamic component. Due to the periodic behavior of the gear mesh, a fine numerical mesh discretization is mandatory to achieve accurate and reliable simulation results in this frequency range [38]. Consequently, a high number of degrees of freedom arises for the housing structure and thus leads to an increase of the computation time. To overcome this issue, a CMS of the housing structure is performed in advance to drastically reduce the number of degrees of freedom for the nonlinear iteration procedure. In contrast to [13], in this paper, primary nodes are only defined for connection points (e.g., bearing locations) and for specific locations of important boundary conditions (e.g., foundation support). All remaining nodes, including all sensor positions, are assigned to the set of secondary nodes and hence are not part of the final computation process. As indicated in [13], computation time reduces drastically, but the storage of the dense transformation matrix with respect to the CMS allocates, in this study, a disk space of almost 5 GB in binary format. Apparently, commercial software packages usually do not (directly) offer such an export option. Consequently, an individual implementation is necessary to recover the physical results of the secondary node set. Accordingly, in this paper, the complete transformation matrix of the CMS is stored and finally employed to the primary node set to retrieve the result of the complete model. Therefore, a global and efficient determination of the housing vibrations (and hence of the ERP density distribution) is simply evaluable. On top, a subsequent (“weakly coupled”) acoustic investigation with the BEM becomes applicable as the velocity information of the complete housing structure is then accessible. In this paper, a direct BEM approach with collocation [17] is applied for the acoustic post-processing of a single gearbox. The interpolation of the physical quantities (sound pressure and sound velocity) is performed with discontinuous constant elements [39]. Sound hard boundary conditions are imposed by zero admittance, which means that the structural velocity perfectly matches the sound velocity on the housing surfaces. To overcome the non-uniqueness problem in exterior domains, the underlying formulation is implemented with respect to [40, 41]. Here, the arising hypersingular integral is numerically solved as suggested by

[42]. However, detailed information regarding further approaches and their corresponding capabilities is available in [43] with respect to acoustic BEM formulations.

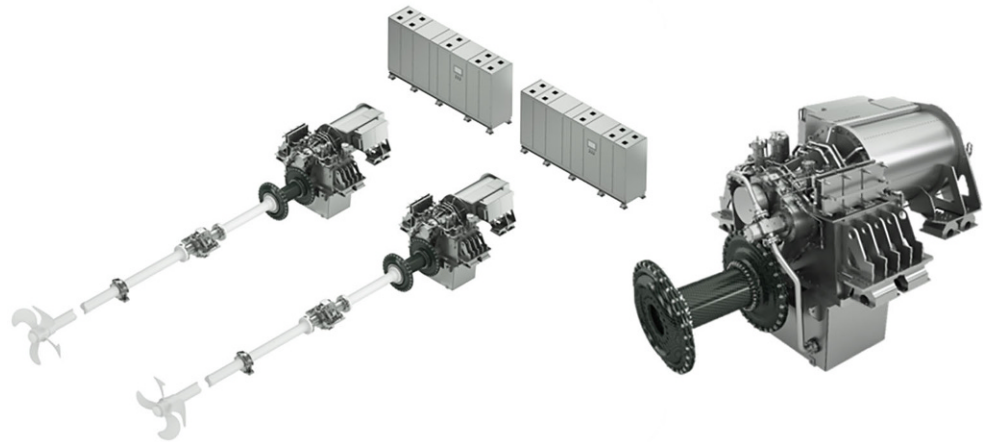
Finally, the nonlinear forced response for a single steady-state operating condition is calculated with the HBM and hence the iterative procedure takes place in the frequency domain. However, to use existing contact formulations, the actual derivation of the nonlinear forces is still performed in the time domain by applying the alternating frequency/time scheme (AFT) [44]. As the convergence behavior of the HBM is quite sensitive, an appropriate initial guess is of major importance. The “sequential continuation” [11] is a common technique for the investigation of a certain speed range. In detail, the result of the preceding operating condition serves as starting point for the next simulation step. To ensure convergence for the first steady-state operating condition, a linear solution is used as the initial guess [13]. This “sequential continuation” scheme is robust as long as no complex behavior (e.g., tooth separation [45]) occurs. For bifurcation analyses and similar, the implementation of the “arc-length method” is highly recommended as described in [46, 47]. Although such complex motions are usually not relevant for this acoustic kind of high performance gears, the “arc-length method” is applied here to ensure a more reliable “path continuation” [11] across the complete speed range. A predictor step in form of a secant through the last two converged operating conditions slightly accelerates the global iteration process.

3 Description of considered gear design concepts

Comparable to the automotive industry, the marine industry is also experiencing an increase in the application of electric motors. As a consequence, the noise characteristics of a gearbox may dominate in a ship propulsion system. A successful solution concept to this modern challenge is illustrated in Fig. 1. Here, a single-stage double-helical gearbox transmits the power of an electric motor to the driving propeller.

Flexible couplings and an elastic foundation support, respectively, build the connection to the adjacent components of the drive train: ship foundation, propeller shaft and drive motor. On this basis, a full elastic separation is assumed at these locations and hence only the gearbox itself is primarily of major interest in the upcoming investigation. In total, the focus is on four different gear designs: A, B, C, and D. All of them are based on the same concept as it is illustrated in Fig. 2, but with different gear design data. The underlying requirement for each gear is a desired transmission capability of 3 MW at a maximum speed of 1000 rpm at the pinion shaft. The output is always located on the opposite

Fig. 1 Schematic overview of an electric ship propulsion system



side at the wheel shaft. Each shaft is supported by two slide bearings and the housing model is rigidly attached at the mounting positions to the ship foundation, see Fig. 4.

The corresponding technical data of the respective gear designs A, B, C, and D are listed in Table 1. While the first three designs share the same center distance of 1050 mm, the shafts of gear unit D only have a center distance of 975 mm. Therefore, gearbox D represents the lightest concept. The face width of one helix is between 110 and 135 mm. To compensate this slight deviation, the span between the slide bearings is adjusted appropriately. The number of teeth is different for all designs and thus the gear mesh excitation frequency is specific for the several versions. While the transverse contact ratio is comparable between all gearboxes, the overlap ratio shows significant differences. This is mainly caused by the variation of the module and the face width as the helix angle is always approx. 30°.

All gears initially include a basic profile modification with respect to maximum strength and power loss behavior, but no acoustic motivation is considered at this point. The actual course of the time varying gear mesh stiffness is illustrated in Fig. 3 for all gear designs over one cyclic period at static operating conditions. The applied torque is

the same for all gear designs and fits the requirement of 3 MW at 1000 rpm pinion speed. During these simulations, the shafts, bearings, and housings behave as rigid bodies and thus do not influence the comparability of these analyses. Finally, the result in Fig. 3 indicates that all designs show a stiffness variation of less than two percent and hence imply at a first glance a comparable excitation behavior.

Moreover, the basic geometry style of the housing structure is identical between all gearboxes. For example, the computational model of version D is illustrated in Fig. 4. For comparability, the intention was to keep the numerical mesh quality and the wall thicknesses the same throughout all four concepts. The only difference is a slight adjustment of the width and length to compensate for the variation of the center distances as well as the bearing spans. In each model, the housing structure is fixed (i.e., a rigid support) at the corresponding overhangs, see Fig. 4.

Usually, quiet operation is not required at maximum speed, but rather at lower speed. Accordingly, the addressed speed range is selected between 300 and 400 rpm. Nevertheless, in order to gain a greater overview with regard to the specific dynamic behavior of the focused gearboxes, the simulations are carried out for a speed range between 250 and 750 rpm. The input torque increases identically for

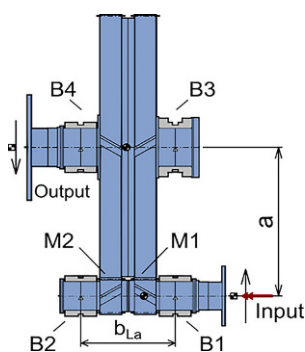


Fig. 2 Basic gear design concept of focused double helical gearboxes A, B, C, and D

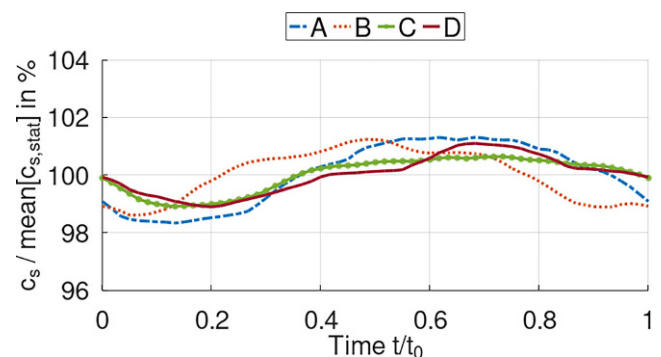


Fig. 3 Time varying gear mesh stiffness as a measure of the expected excitation characteristics of gearboxes A, B, C, and D

Fig. 4 Housing design of focused gearboxes with respect to the applied FE-model

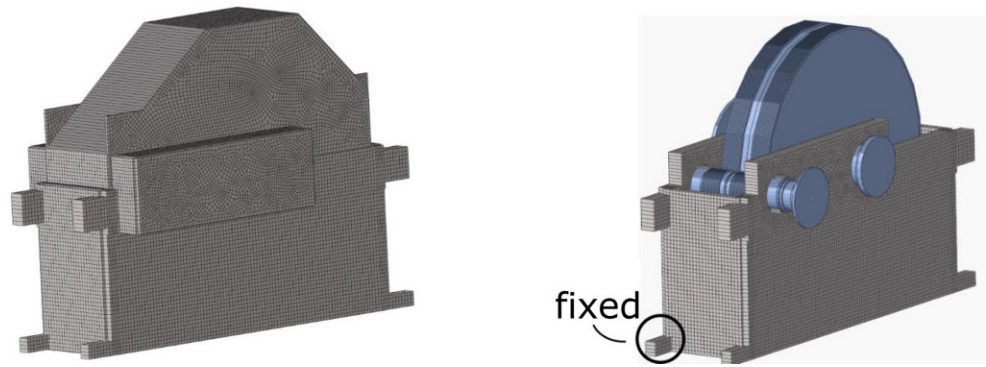


Table 1 Technical data of focused double helical gearboxes A, B, C, and D

Gearbox	–	–	A	B	C	D
Module	M_n	mm	9.0	7.0	5.5	7.0
Pressure angle	α_n	°	20.0	20.0	20.0	20.0
Helix angle	β	°	± 28.9	± 31.3	± 30.7	± 31.2
Number of teeth	Z_p/z_w	–	23/181	29/227	37/291	27/211
Transverse contact ratio	ϵ_a	–	1.38	1.37	1.41	1.36
Overlap ratio	ϵ_b	–	1.95	2.63	3.97	3.10
Face width (one helix)	b	mm	114.0	111.5	134.5	131.5
Center distance	a	mm	1050.0	1050.0	1050.0	975.0
Bearing span	b_{La}	mm	557.0	540.0	578.0	579.0
Total mass	m	t	13.7	13.3	14.2	12.7

each gearbox as shown in Fig. 5. The course represents a conventional behavior of a propeller system. Additionally, deadweight contributes to this constant external load. There are no external excitations considered in this model and thus only the power transmission process of the mating gear teeth induces all forced vibrations as an internal excitation component.

At this point, it is also noteworthy to mention that none of these gearboxes actually exists. With respect to the total weight, the wheel body may usually also come in a more complex lightweight design. Even though this type of calculation is possible with the applied methodology, it is deliberately omitted here in order to suppress additional influences and to keep the complexity of the dynamic model as low as possible. Nevertheless, all these concepts fulfill in

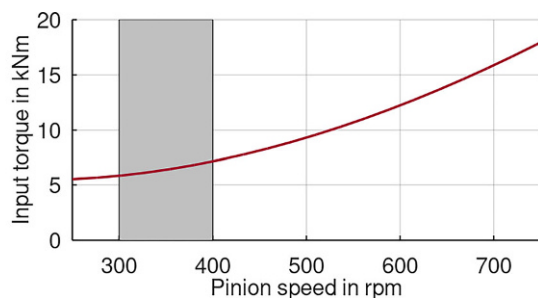


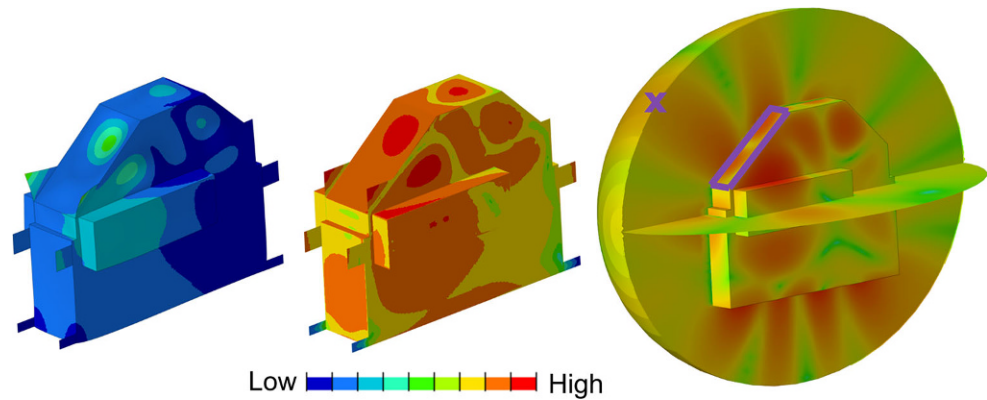
Fig. 5 Increase of the input torque at the pinion shaft for all focused gearboxes

general the mechanical requirements and hence are realistic options for production without any restrictions.

4 Application and results

In general, one computational model holds more than 500k degrees of freedom and six nonlinearities: two gear meshes (M1/M2) and four slide bearings (B1–B4). However, the computation time for a single steady-state analysis on a CAD workstation (Intel i9-9920X CPU @ 3.50GHz, 2×12 Cores) is only five minutes. A subsequent acoustic post-processing of these structural vibrations by means of the BEM takes additional 15 min for each operating condition to compute the sound pressure for about 30k constant elements on the housing surfaces. An example result in form of a forced vibration response is illustrated in Fig. 6 for gearbox D at 750 rpm. On the left hand side, the global deformation behavior of the housing structure is indicated. Additionally, in center position, the distribution of the ERP densities is given and on the right hand side, the generated sound pressure is illustrated on the housing surfaces as well as in the surrounding fluid domain. Critical surface areas regarding sound radiation are identified by this observation. A first comparison between the deformation vibration, the ERP densities, and the sound pressure distribution seems to be meaningful.

Fig. 6 Forced vibration of gearbox D at 750 rpm (*left*); Density distribution of equivalent radiated power (ERP) of gearbox D at 750 rpm (*center*); Distribution of sound pressure level (SPL) of gearbox D at 750 rpm (*right*)



On that note, in Fig. 7, the equivalent radiated power (ERP) of the top surface (see rectangle in Fig. 6, right) is compared to the corresponding actual radiated sound power (RSP) for gearbox D across the full speed range. In addition, the dynamic behavior of the sound pressure level (SPL) of one representative virtual microphone (see cross mark in Fig. 6, right) is also given. To acknowledge the human perception of sound, an A-weighting is employed to all results. The ERP as well as the RSP represent absolute values and a direct comparability is granted. In contrast, the reference value of the SPL is adjusted to fit the range of the sound power levels. Therefore, the given SPL allows only a qualitative interpretation of the dynamic resonance behavior between specific operating conditions.

With respect to Fig. 7, the ERP slightly overestimates the actual radiated sound power, but, in total, provides meaningful absolute values. This finding coincides with the observations in [15, 17], where a similar study is made on a diesel engine. In contrast, the SPL shows higher deviations with respect to the basic resonance behavior in specific speed ranges. For example, at about 475 rpm, the calculated SPL indicates a similar noise level as given at 400 rpm, while the ERP exhibits a significant decrease from 400 to 475 rpm. However, the general course of the SPL is also in an acceptable agreement with the dynamic behavior of the ERP and thus, the ERP is selected due to efficiency reasons as

the reference criteria in the upcoming simulations to assess the acoustic performance of a gearbox.

The calculated forced response deformations are absolute values that arise from a mechanical simulation of the power transmission process. As a result, this output is directly concrete and hence allows a straight comparison between different gear designs with respect to noise generation. This simulation strategy enables a cross evaluation over completely different gear design concepts as it predicts quantitative parameters instead of qualitative ones.

On that note, the derived ERP values of the top housing surface (see rectangle in Fig. 6, right) are again scaled by an A-weighting to acknowledge the human perception of sound. This scaling procedure is intended to harmonize the varying frequency content between the different gear designs with respect to the gear mesh period. The results for all gear designs are shown in Fig. 8 for the addressed speed range between 250 and 750 rpm. A direct comparison is possible.

In the specific speed range between 300 and 400 rpm, gearbox A in total shows the best acoustic performance. In contrast, the smallest gearbox D indicates the highest sound radiation at about 375 rpm. The fact that gearbox A has the smallest overlap ratio and a relatively high excitation level, but, however, shows the best running smoothness, confirms that the transfer path (with respect to the mesh frequency) has a significant influence on the transportation of the struc-

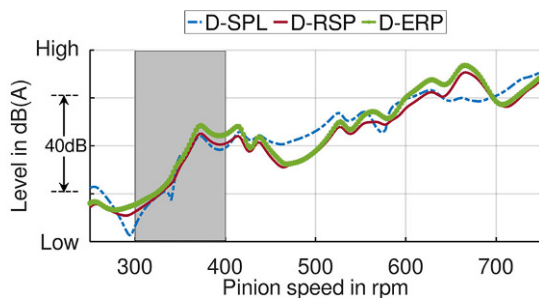


Fig. 7 Dynamic behavior of sound pressure level (SPL), radiated sound power (RSP), and equivalent radiated power (ERP) of gearbox D

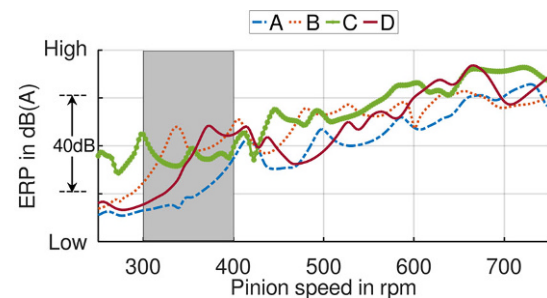
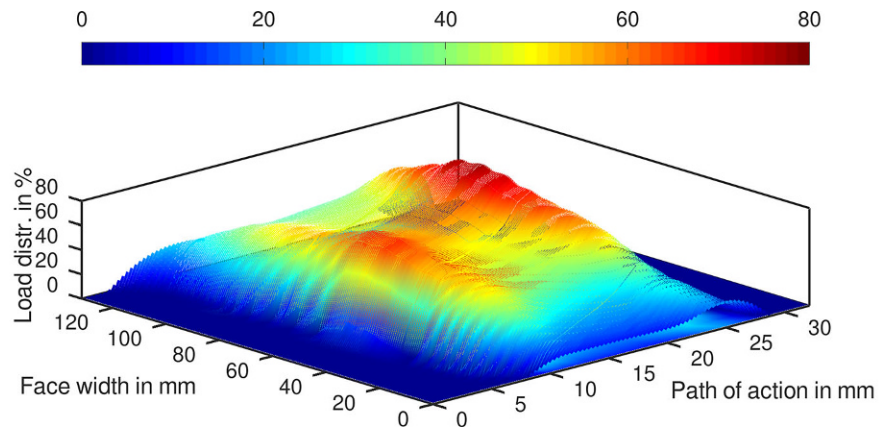


Fig. 8 Equivalent radiated power (ERP) of focused gearboxes A, B, C, and D

Fig. 9 Dynamic load distribution of gear mesh M1 in gearbox D at 750rpm



ture-borne sound. In other words, the gear mesh excitation is transmitted extremely “effectively” from the dynamic system to the housing surfaces in gearbox D for this specific speed range. The addressed resonance of gearbox D at about 375 rpm corresponds to an excitation frequency of the gear mesh of about 170 Hz. At this frequency, the dynamic model holds a mode shape which is mainly located in the housing structure. Similar mode shapes in this frequency range are also found for the other gear concepts since the basic geometry of all gearboxes is intentionally very similar. As a result, this resonance establishes in all gearboxes. Referring to Fig. 8, gearbox A shows an appropriate forced vibration response at about 415 rpm, gearbox B at about 335 rpm, and gearbox C at about 260 rpm. All these peaks are on a close level, but still exhibit differences with respect to various design definitions as well as to the course of the applied torque (Fig. 5).

However, to investigate this behavior in more detail, an acoustically optimized profile modification is developed for gearbox D. For this purpose, the dynamic load distribution is taken as a reference criteria. In contrast to the static stiffness behavior (Fig. 3), the elastodynamic contribution of the surrounding components is included nonlinear and thus a concrete statement regarding the actual impact on the dynamic excitation behavior in the total system is accessible.

Fig. 10 Dynamic load distribution of gear mesh M1 in gearbox D at 750rpm with optimized profile modifications

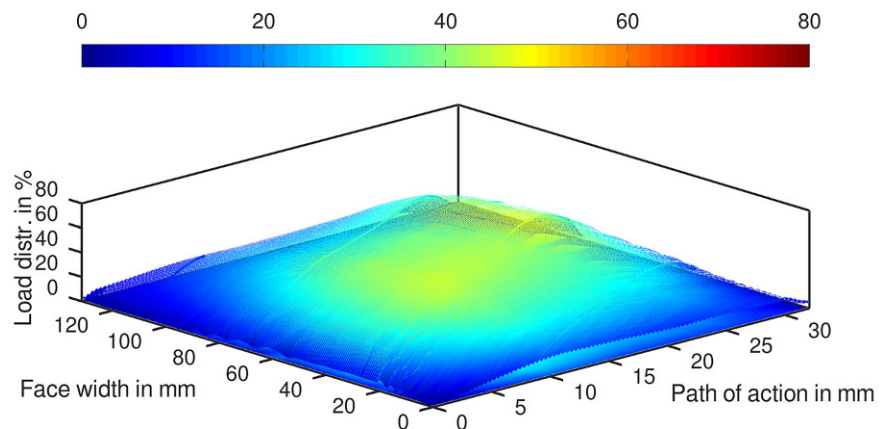


Figure 9 shows the dynamic load distribution (related to the analytical mean value) on the tooth flanks of gear mesh M1 in gearbox D for 750 rpm with the standard reference profile modification. In contrast, the corresponding result for the optimized modification is illustrated in Fig. 10. Both Figures are colored with respect to the same legend in order to achieve a direct comparability. A smoother running operation is clearly indicated.

Finally, in Fig. 11, the additional result of the optimized gear design D-optimized is illustrated next to the original gear design A and next to the original gear design D. A total reduction of the noise level is perceived for the optimized gearbox D as compared to its original design D. Thus, the positive effectiveness of this profile modification across the complete speed range is confirmed. However, at almost 450 rpm the optimized profile modification does not provide any benefit in relation to the original concept. On top, the optimized version of gearbox D shows still a higher noise radiation ability than gearbox A in the specific speed range between 350 and 400 rpm.

This investigation of the sound and vibration behavior demonstrates the effectiveness of primary measures. Additionally, this design study represents a kind of secondary measure since the dynamic transfer path for a specific application is optimized by various design alternatives. A com-

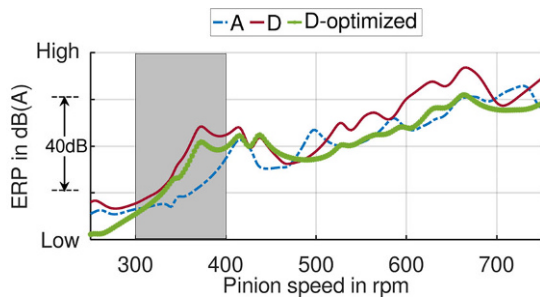


Fig. 11 Equivalent radiated power of gearbox A, D, and D with an optimized profile design

bination of both approaches is a recommendable strategy to meet the requirements of a modern transmission system.

5 Conclusions

This paper demonstrates the importance of an appropriate total system analysis with respect to acoustically motivated investigations and challenges. Using the harmonic balance method, both, noise excitation and noise transmission through the casing may be considered efficiently in the design phase to evaluate the acoustic behavior of a gearbox. Comparative example calculations confirm that the complete system needs to be considered to tell the difference between competitive design variants.

Future research will focus on the detection of important influencing factors in combination with parameter studies. Moreover, the conducted acoustic investigation with the boundary element method provides motivation for a more detailed survey on the equivalent radiated power with respect to the actual radiated sound pressure levels.

Funding Open Access funding enabled and organized by Projekt DEAL.

Conflict of interest A. Beinstingel, F. Haringer, W. Sigmund, M. Heider, B. Pinnekamp and S. Marburg declare that they have no competing interests.

Open Access This article is licensed under a Creative Commons Attribution 4.0 International License, which permits use, sharing, adaptation, distribution and reproduction in any medium or format, as long as you give appropriate credit to the original author(s) and the source, provide a link to the Creative Commons licence, and indicate if changes were made. The images or other third party material in this article are included in the article's Creative Commons licence, unless indicated otherwise in a credit line to the material. If material is not included in the article's Creative Commons licence and your intended use is not permitted by statutory regulation or exceeds the permitted use, you will need to obtain permission directly from the copyright holder. To view a copy of this licence, visit <http://creativecommons.org/licenses/by/4.0/>.

References

- Hoppe F, Pinnekamp B (2004) Gear noise—Challenge and success based on optimized gear geometries. In: AGMA Fall Technical Meeting 2004; Milwaukee, WI, 25/26 October, 2004
- Özgiiven HN, Houser DR (1988) Mathematical models used in gear dynamics—A review. *J Sound Vib* 121(3):383–411
- Ambarisha VK, Parker RG (2007) Nonlinear dynamics of planetary gears using analytical and finite element models. *J Sound Vib* 302(3):577–595
- Cooley CG, Parker RG, Vijayakar SM (2011) A frequency domain finite element approach for three-dimensional gear dynamics. *J Vib Acoust* 133(4):041004 (9 pages). <https://doi.org/10.1115/1.4003399>
- Velex P (2012) On the modelling of spur and helical gear dynamic behaviour. In: Gokcek M (ed) *Mechanical engineering*. IntechOpen, pp 75–106
- Dai X, Cooley CG, Parker RG (2019) An efficient hybrid analytical-computational method for nonlinear vibration of spur gear pairs. *J Vib Acoust* 141(1):11006
- Kang M, Kahraman A (2021) An experimental and theoretical study of quasi-static behavior of double-helical gear sets. *J Mech Des* 143(4):43401
- Chimanpure AS, Kahraman A, Talbot D (2021) A transient mixed elastohydrodynamic lubrication model for helical gear contacts. *J Tribol* 143(6):15
- Guo Y, Eritenel T, Ericson TM, Parker RG (2014) Vibro-acoustic propagation of gear dynamics in a gear-bearing-housing-system. *J Sound Vib* 333(22):5762–5785
- Han J, Liu Y, Yu S, Zhao S, Ma H (2021) Acoustic-vibration analysis of the gear-bearing-housing coupled system. *Appl Acoust* 178(13):108024
- Krack M, Gross J (2019) *Harmonic balance for nonlinear vibration problems*, 1st edn. Springer, Berlin
- Mélot A, Perret-Liaudet J, Rigaud E (2022) Vibro-impact dynamics of large-scale geared systems. *Nonlinear Dyn* 111:4959–4976
- Beinstingel A, Schabert S, Heider M, Pinnekamp B, Marburg S (2023) Computational prediction of structure-borne noise in a two stage double-helical gearbox using harmonic balance method. *Mech Syst Signal Process* 189:110112
- Craig RR Jr., Bampton MC (1968) Coupling of substructures for dynamic analyses. *AIAA J* 6(7):1313–1319
- Fritze D, Marburg S, Hardtke H-J (2009) Estimation of radiated sound power: A case study on common approximation methods. *Acta Acust United Acust* 95:833–842
- Luegmair M, Muench H (2015) Advanced equivalent radiated power (ERP) calculation for early vibro-acoustic product optimization. In: *International Conference on Sound and Vibration (Florence, Italy) ICSV22*, p 8
- Kaltenbacher M (2017) *Computational acoustics*. Springer, Heidelberg
- Nelson HD (1980) A finite rotating shaft element using timoshenko beam theory. *J Mech Des* 102(4):793–803
- Greenhill LM, Bickford WB, Nelson HD (1985) A conical beam finite element for rotor dynamics analysis. *J Vib Acoust* 107(4):421–430
- Cowper GR (1966) The shear coefficient in Timoshenko's beam theory. *J Appl Mech* 33(2):335–340
- Reynolds O (1886) On the theory of lubrication and its application to Mr. Beauchamp Tower's experiments including an experimental determination of the viscosity of olive oil. *Philos Trans R Soc Lond* 177:157–234
- Argyris J, Scharpf D (1970) Finite element formulation of the incompressible lubrication problem. *Nucl Eng Des* 11(2):225–229
- Gümbel L (1914) *Das Problem der Lagerreibung*. Merkblatt Bezirksverband Deutscher Ingen. VDI, vol 5, pp 87–104

24. Beinstingel A, Keller M, Heider M, Pinnekamp B, Marburg S (2021) A hybrid analytical-numerical method based on isogeometric analysis for determination of time varying gear mesh stiffness. *Mech Mach Theory* 160:104291
25. Beinstingel A, Heider M, Pinnekamp B, Marburg S (2021) Gear mesh excitation and non-uniform rational b-splines. *Forsch Ingenieurwes* 86:331–336
26. Weber C, Banaschek K (1953) Formänderung und Profilrücknahme bei gerad- und schrägverzahnten Rädern. *Schriftenreihe Antriebstechnik*, vol 11, pp 1–88
27. Schmidt G (1972) Berechnung der Wälzpressung schrägverzahnter Stirnräder unter Berücksichtigung der Lastverteilung (Dissertation, Technical University of Munich, Munich)
28. Conry TF, Seireg A (1973) A mathematical programming technique for the evaluation of load distribution and optimal modifications for gear systems. *J Eng Ind* 95(4):1115–1122
29. Neupert B (1983) Berechnung der Zahnkräfte, Pressungen und Spannungen von Stirn- und Kegelradgetrieben (Dissertation, RWTH Aachen, Düsseldorf)
30. Chang L, Liu G, Wu L (2015) A robust model for determining the mesh stiffness of cylindrical gears. *Mech Mach Theory* 87:93–114
31. Cottrell JA, Hughes TJ, Bazilevs Y (2009) *Isogeometric analysis: toward integration of CAD and FEA*. John Wiley & Sons
32. Marafona JDM, Marques PMT, Martins RC, Seabra JHO (2021) Mesh stiffness models for cylindrical gears: A detailed review. *Mech Mach Theory* 166:104472
33. Sainsot P, Vex P (2020) On contact deflection and stiffness in spur and helical gears. *Mech Mach Theory* 154:104049
34. Baethge J (1969) Drehwegfehler, Zahnfederhärte und Geräusch bei Stirnrädern (Dissertation, TH Munich, Munich)
35. Thoma FA (2012) Lastübertragung im verformten System Lager-Welle-Zahnrad (Dissertation, Technical University of Munich, Munich)
36. Gerber H (1984) Innere dynamische Zusatzkräfte bei Stirnradgetrieben (Dissertation, Technical University of Munich, Munich)
37. Strutt JW, Rayleigh B (1878) *The theory of sound*, 1st edn. vol II. Macmillan, London
38. Langer P, Maeder M, Guist C, Krause M, Marburg S (2017) More than six elements per wavelength: The practical use of structural finite element models and their accuracy in comparison with experimental results. *J Comput Acoust* 25(04):1750025
39. Rego Silva JJ, Wrobel LC, Telles JCF (1993) A new family of continuous/discontinuous three-dimensional boundary elements with application to acoustic wave propagation. *Int J Numer Meth Engng* 36:1661–1679
40. Burton AJ, Miller GF (1971) The application of integral equation methods to the numerical solution of some exterior boundary-value problems. *Proc R Soc Lond* 323:201–220
41. Marburg S (2016) The Burton and Miller method: Unlocking another mystery of its coupling parameter. *J Comput Acoust* 24:1550016
42. Guiggiani M, Krishnasamy G, Rudolphi TJ, Rizzo FJ (1992) A general algorithm for the numerical solution of hypersingular boundary integral equations. *ASME J Appl Mech* 59:604–614
43. Preuss S, Gurbuz C, Jelich C, Baydoun SK, Marburg S (2022) Recent advances in acoustic boundary element methods. *J Theor Comput Acoust* 30(3):2240002
44. Cameron TM, Griffin JH (1989) An alternating frequency/time domain method for calculating the steady-state response of nonlinear dynamic systems. *J Appl Mech* 56:149–154
45. Celikay A, Donmez A, Kahraman A (2021) An experimental and theoretical study of subharmonic resonances of a spur gear pair. *J Sound Vib* 515:116421
46. Mélot A, Rigaud E, Perret-Liaudet J (2022) Bifurcation tracking of geared systems with parameter-dependent internal excitation. *Nonlinear Dyn* 107:413–431
47. Colaitis Y, Batailly A (2021) The harmonic balance method with arc-length continuation in blade-tip/casing contact blades. *J Sound Vib* 502:116070